JBC Papers in Press. Published on May 24, 2017 as Manuscript M117.775700
The latest version is at http://www.jbc.org/cgi/doi/10.1074/jbc.M117.775700

Protein Kinase C ε Stabilizes β-Catenin and Regulates Its Subcellular Localization in Podocytes

Michelle Duong[1], Xuejiao Yu[1], Beina Teng[1], Patricia Schroder[2], Hermann Haller[1], Susanne Eschenburg[3] and Mario Schiffer[1]

[1]From the department of Hypertension and Nephrology, Hanover Medical School, 30625 Hanover, Germany

[2]From Mount Desert Island Biological Laboratory, P.O. Box 35, Old Bar Harbor Road, Salisbury Cove, ME 04672, USA

[3]From the Institute for Biophysical Chemistry, Hanover Medical School, 30625 Hanover, Germany

Running title: Regulation of β-Catenin by PKCε

To whom correspondence should be addressed: Prof. Dr. med. Mario Schiffer, Department of Hypertension and Nephrology, Carl-Neuberg-Strasse 1, 30625 Hanover, Germany; Tel. (0511) 5323666; Email: schiffer.mario@mh-hannover.de

Keywords: Wnt pathway, beta-catenin (β-catenin), protein kinase C (PKC), kidney, cytoskeleton, glycogen synthase kinase 3 (GSK3), cadherin, podocytes

ABSTRACT

Kidney disease has been linked to dysregulated signaling *via* protein kinase C (PKC) in kidney cells such as podocytes. PKCα is a conventional isoform of PKC and a well-known binding partner of β-catenin, which promotes its degradation. β-Catenin is the main effector of the canonical Wnt pathway and is critical in cell adhesion. However, whether other PKC isoforms interact with β-catenin has not been studied systematically. Here we demonstrate that PKCε-deficient mice, which develop proteinuria and glomerulosclerosis, display a lower β-catenin expression compared to PKC wildtype mice, consistent with an altered phenotype of podocytes in culture. Remarkably, β-catenin showed a reversed subcellular localization pattern: while β-catenin exhibited a perinuclear pattern in undifferentiated wild-type cells, it predominantly localized to the nucleus in PKCε-knockout cells. Phorbol 12-myristate 13-acetate stimulation of both cell types revealed that PKCε positively regulates β-catenin expression and stabilization in a glycogen synthase kinase-3β independent manner. Further, β-catenin overexpression in PKCε-deficient podocytes could restore the wildtype phenotype, similar to the rescue with a PKCε construct. This effect was mediated by upregulation of P-cadherin and the β-catenin downstream target fascin1. Zebrafish studies indicated three PKCε-specific phosphorylation sites in β-catenin that are required for full β-catenin function. Co-immunoprecipitation and pulldown assays confirmed PKCε and β-catenin as binding partners and revealed that ablation of the three PKCε phosphorylation sites weakens their interaction. In summary, we identified a novel pathway for regulation of β-catenin levels and define PKCε as an important β-catenin interaction partner and signaling opponent of other PKC isoforms in podocytes.

INTRODUCTION

The Protein Kinase C (PKC) family of serine- and threonine kinases is subdivided into the three subfamilies of conventional, atypical, and novel PKCs (1), depending on the involvement of diacyglycerol (DAG) and calcium during activation. Conventional, atypical and novel PKCs display different roles in signal transduction via phosphorylation of their target proteins. Regarding the kidney, several studies have shown that PKCs play a pivotal role in the development of diabetic nephropathy. For PKCα and PKCβ, two members of the conventional PKC subfamily, a complete depletion seems to lead to a better outcome in streptozotocin-induced diabetic mice in terms of proteinuria (2) or renal hypertrophy and glomerular injury (3). This

implies that these PKC isoforms induce or exacerbate kidney injury. In contrast, we have previously shown that knockdown of PKCε in mice leads to a renal phenotype with glomerulosclerosis, indicating that PKCε may protect from diabetic nephropathy (4, 5).

PKCε belongs to the subfamily of novel PKCs and is activated via DAG, different from conventional isoforms, which are activated by calcium and DAG. PKCε was previously shown to play an essential role in cell proliferation, migration, invasion and survival, and the lack of PKCε is linked to reduced cardioprotective effects (6) and neurotransmission (7). Moreover, PKCε has been well characterized as an important binding protein of actin and thus has regulatory function for the cytoskeleton (8, 9).

β-Catenin is the key component in the highly conserved canonical Wnt pathway, regulating cell-cell adhesion as well as serving as a transcription co-factor (10). Widely expressed, β-catenin is also found in podocytes and plays a pivotal role in cell adhesion and differentiation. Depending on phosphorylation, β-catenin exists in an active (non-phosphorylated) and an inactivated (phosphorylated) state. Early studies demonstrated that overexpression of β-catenin alone can cause or aggravate damage in podocytes (11), while in apparent contradiction, a later study showed, that β-catenin-knockout mice under diabetic conditions display more albuminuria than control mice in long-term studies (>15 weeks) (12). From their conflicting data, *Kato et al.* went on to show that a balanced expression of active and inactive β-catenin might be what is important for the cell function (12).

The presence of β-catenin is strongly regulated via glycogen synthase kinase-3β (GSK3β), which forms a degradation complex with APC, Axin and CK-1 upon Wnt absence. The resulting N-terminal phosphorylation of β-catenin leads to ubiquitination and proteasome-mediated reduction of cellular β-catenin level.

In contrast, activation of Wnt, a group of secreted glycolipoproteins, leads to stabilization and accumulation of β-catenin in the cytoplasm and translocation into the nucleus, which then results in Wnt target gene expression (13).

Other so-called non-canonical Wnt signaling pathways, especially the Wnt/Ca^{2+} pathway, are involved in PKC signaling (14); many studies have demonstrated the alternative degradation of β-catenin by PKC isoforms such as PKCα (15, 16). PKCα has been shown to mediate a GSK3β independent β-catenin downregulation by phosphorylation of the N-terminal serine residues S33, S37 and S45 of β-catenin. This finding is consistent with the known common phosphorylation sites of GSK3β (17).

The aim of this study was to analyze the relationship between β-catenin and PKCε in podocytes. We used a murine PKCε knockout podocyte cell line to perform *in vitro* immunofluorescence staining, characterize the β-catenin expression under Phorbol 12-myristate 13-acetate (PMA) stimulation and adenoviral constructs to investigate the effects of an overexpression of β-catenin in PKCε knockout podocytes. Furthermore, we created β-catenin mutants and validated these *in vitro* and *in vivo* to investigate which domain of β-catenin may contribute to the interaction/function with PKCε.

RESULTS

PKCε knockout in mice leads to proteinuria and reduced expression of β-catenin - To evaluate podocytic expression of β-catenin in mice we performed immunofluorescence costaining of the podocyte marker synaptopodin and β-catenin on glomeruli of 12-week wildtype and PKCε -/- mice. β-Catenin expression was detected in the nucleus as well as in the cytoplasm in wildtype mice, whereas in PKCε -/- glomeruli we observed a predominantly nuclear localization. Further, the β-catenin expression was less intense in PKCε -/- than in wildtype mice (Fig. 1A). Semiquantitative analysis of β-catenin of fluorescent cells in the glomeruli of the mice (≥10 glomeruli were included for each genotype) confirmed that β-catenin expression in WT mice was significantly higher than in PKCε -/- mice at 12 weeks of age (Fig.1B, ****$p < 0.0001$). Of note, Coomassie staining of urine revealed that the glomerular barrier function was already impaired, displaying a mild albuminuria onset at 12 weeks of age in the PKCε deficient mice (Fig. 1C).

PKCε influences the subcellular distribution of β-catenin and its activity - Since we detected a difference in podocytic β-catenin expression between glomeruli of wildtype and PKCε -/- mice, we wanted to investigate the expression *in vitro* in wildtype and PKCε -/- podocytes. Interestingly, the PKCε -/- podocytes displayed a

very unique phenotype in tissue culture, as they were significantly smaller than the wildtype podocytes, detached very easily and never reached a confluent growth pattern. Western blot analysis using antibodies against active and total β-catenin showed similar results as those *in vivo*, displaying an increased expression from d0 to d10 (Fig. 2A), with a stronger upregulation in wildtype cells than in the knockout cells. The upregulation supported findings in other cell lines (18, 19), which indicated that the presence of β-catenin is critical for cell differentiation. An immunofluorescent staining timecourse (0d, 4d, and 8d after differentiation) revealed a reverse localization of β-catenin in wildtype and PKCε -/- podocytes during differentiation (Fig. 2B). In wildtype cells, the localization of β-catenin expression changed from a predominant expression in the perinuclear areas, exhibited at d0, to expression in the nuclei and the cell junctions during differentiation (at d4, d8). In contrast, β-catenin in PKCε -/- podocytes translocated from the nuclei (d0) to the perinuclear areas and cell junctions (d4, d8). We quantified the shift and intensity of the localization of β-catenin by expressing the ratio of the mean fluorescence of the nuclei in relation to the perinuclear areas. The quantification supported the observation that β-catenin expression changes significantly from perinuclear areas to nuclei in wildtype podocytes during differentiation (Fig.2B/C, ****$p < 0.0001$), whereas in PKCε -/- podocytes, β-catenin switches from nuclei to perinuclear areas (Fig. 2 B/C ***$p < 0.0002$). These data suggest that PKCε orchestrates the subcellular localization of β-catenin in podocytes, which significantly shifts during a differentiation time course (d0 and d8; ****$p < 0.0001$ and *$p < 0.05$). Interestingly, at d4 no difference was observed between both genotypes implying a PKCε dependent checkpoint of β-catenin during podocyte differentiation.

PKCε stabilizes active β-catenin levels in a GSK3β-independent manner - To further explore the effects of PKCε on β-catenin activity, PMA – a reversible and highly potent PKC activator – was used to stimulate murine wildtype and PKCε knockout podocytes. Normalization of Western blot results indicated that after differentiation for 8 days, PMA stimulation for 30 minutes and 1, 2, 4, 8 and 24 hours results in an increase of active (non-phosphorylated) β-catenin in wildtype podocytes (Fig. 3A) up to 2 h, followed by continuous reduction over the 24-hr time course. In contrast, PKCε -/- podocytes showed no temporary upregulation of β-catenin, instead we noted a gradual diminishment of active β-catenin from the start of the timecourse to its end, indicating an accelerated degradation of active β-catenin in PKCε -/- podocytes. The impact of the PMA stimulation on active β-catenin expression was significantly higher (*$p < 0.05$, **$p < 0.01$) in wildtype podocytes than in PKCε-deficient cells (Figure 3B).

To investigate whether the diminished β-catenin levels resulted from a rising activation of GSK3β, the main inhibitor of the canonical Wnt pathway, we analyzed GSK3 activity after PMA stimulation. GSK3β levels were detected at a constant expression level in both wild type and PKCε knockout podocytes (Fig. 3C/D). Since the phosphorylation level of GSK3 α/β at S9/21, leads to decreased activity (20) we also looked at p-GSK3 after PMA stimulation. p-GSK3β increased in both groups in a similar fashion during the time course (Fig. 3C), indicating that the reduced β-catenin expression in the PKCε -/- podocytes is independent of GSK3β expression and activity.

β-Catenin overexpression rescues the impaired actin cytoskeleton of PKCε deficient podocytes - As previously shown (21), PKCε deficient murine podocytes in culture display a malfunction in the organization of the actin cytoskeleton. F-Actin and focal adhesion marker paxillin staining revealed an overall smaller cell size, less stress fibers and reduced size and number of focal adhesions in PKCε -/- podocytes. (Fig. 4A). The adenoviral transduction with a PKCε-wildtype construct in PKCε deficient podocytes indicated a complete rescue of the phenotype as expected, and the cells displayed a rearranged cytoskeleton and higher levels of paxillin. Interestingly, adenoviral transduction with wildtype-β-catenin construct in PKCε-knockout cells led to a similar recovery as the rescue with the PKCε-wildtype construct. Measurement of the average cell size performed with ImageJ demonstrates PKCε-knockout cells transfected with PKCε and β-catenin reach cell sizes similar to PKC-wildtype cells and a similar distribution pattern of paxillin expression with elongated focal contacts (Fig. 4A/B).

Since β-catenin plays a major role in cell adhesion with its binding partner P-cadherin (22) and the PKCε-knockout podocytes in culture detach very

easily, we examined the impact of PKCε deficiency on P-cadherin expression during cell differentiation. As depicted in Fig. 4C, P-cadherin expression was drastically reduced in the knockout cells. As expected, we could restore normal P-cadherin expression by overexpressing a wildtype-PKCε construct (Fig. 4D/E). Interestingly, overexpressing a wildtype-β-catenin construct in the PKCε-knockout podocytes also led to a significant increase of P-cadherin expression (* $p < 0.05$), which was not detected in cells transduced with a pAd-Dest vector alone.

To explore how the actin cytoskeleton is restored by β-catenin, we considered known protein targets of β-catenin that are downstream in the Wnt pathway which may interfere with the cytoskeleton. This led us to discover reduced mRNA expression levels of fascin1 in PKCε deficient podocytes. The fascin1 level significantly increased when cells were transduced with either a PKCε or a β-catenin construct (Fig. 4F). Fascin1, an actin filament-bundling protein (23), is known to bind to β-catenin at the cellular edges and possesses a PKC binding site at serine 39 (24, 25). Western blot analysis of lysates from the adenovirus-transfected cells confirmed the qRT-PCR results. (Fig. 4G/H). The knockout cells that were rescued by overexpression of PKCε or β-catenin exhibited a significantly higher fascin1 protein expression than the mock-(pAd-Dest)-transduced PKCε -/- podocytes (p** < 0.05). These data suggest that β-catenin mediates the podocytic actin cytoskeleton via regulation of fascin1 expression.

PKCε specific phosphorylation sites in β-catenin are indispensable for filtration barrier function - After the discovery that β-catenin and PKCε expression levels influence each other, we wanted to explore whether PKCε is a binding partner of β-catenin as previously reported for PKCα (15, 16). To this end, we performed co-immunoprecipitation experiments in HEK cells transfected with GFP-tagged PKCε (or PKCα as a positive control) and FLAG-tagged β-catenin constructs. Indeed, after immunoprecipitation of FLAG-tagged β-catenin we detected an interaction with PKCε as well as with PKCα (Fig.5A).

To further characterize whether the interaction between PKCε and β-catenin derives from a direct or indirect linkage, we performed a pulldown assay with pure recombinant GST-β-catenin and His-PKCε. These experiments confirmed a direct interaction between the two proteins *in vitro* (Fig. 5B).

To elucidate which domain of β-catenin is important and functionally altered by its interaction with PKCε, we searched for specific phosphorylation sites with Phospho-motif-predicting programs such as PhosphoNET, HPRD release 9, dbPTM 3.0, SysPTM 2.0 and UniProt. We chose seven phospho-motifs with matches in at least three databases (Fig. 5C). We performed site-directed mutagenesis to ablate these phosphorylation sites in β-catenin (the amino acid serine was either mutated to alanine or arginine, and threonine was switched to alanine) and performed zebrafish experiments to explore the biological relevance of these mutations of potential PKCε binding sites. To accomplish this, we first established the knockdown model of zebrafish β-catenin1 expression using a β-catenin1 morpholino. Zebrafish express two isoforms of β-catenin, which seem to be functionally redundant during the development (26). We decided to use specific morpholinos for the β-catenin1 isoform for our knockdown experiments, since there is a significantly higher percentage of sequence similarity of this isoform to the mammalian and Xenopus protein sequences (27). As depicted in Fig. 5D, the reduction of β-catenin in zebrafish leads to a phenotype with edema of the yolk sac, pericardial effusion and a shorter tail compared with control morpholino injected fish. The dorsalized phenotype thus displayed typical features of the β-catenin1 knockdown, also seen in other studies (26, 27). Using our previously described eye assay, we measured the level of proteinuria in zebrafish larvae (28). In brief, the eye assay is an indirect method for determining proteinuria. The experimental zebrafish are transgenic for a liver promoter-driven GFP-labeled vitamin-D-binding protein with a molecular weight of 78kD, which accumulates in the circulation under normal conditions and can be easily quantified in the retinal blood vessel plexus of the fish. Decreased fluorescence levels, as displayed by the β-catenin knockdown fish indicated a significant loss of high molecular weight proteins from the circulation of the fish (Fig. 5E). To verify the specificity of the β-catenin1 knockdown, we also performed a cross-species rescue experiment with a wildtype mRNA construct, leading to full recovery of the proteinuria phenotype (Fig. 5E). Next, we performed cross-species rescue experiments by co-injecting the β-catenin

zebrafish morpholino and cRNA of different murine β-catenin mutant constructs. The mutants S47R, T551A/S552A, S675A and S715R/S718A showed a partial or full rescue of the proteinuria phenotype with increased levels of circulating fluorescence in the fish. The rescue was considered partial when the mean fluorescence level was significantly higher than the β-catenin-knockdown zebrafish (* $p > 0.05$), and full when the statistical significance was ***$p < 0.001$. In contrast, the mutants S352R, T472A/S473R and S663A were not able to rescue the β-catenin phenotype, indicating a functional role of these phosphorylation sites. Interestingly, co-immunoprecipitation experiments using anti-FLAG-beads and HEK cells transfected with GFP-tagged PKCε and with these FLAG-tagged β-catenin mutants also confirmed a lower binding affinity in the β-catenin mutants that did not exhibit rescue activity in the zebrafish experiments (Fig. 5F). These observations indicated that the ablated phosphorylation sites are relevant for the interaction between PKCε and β-catenin *in vivo and in vitro*. As a control to ensure the constructs would not influence the glomerular filtration function, we also performed overexpression of all constructs in developing fish larvae and detected no difference in fluorescence levels compared to scrambled morpholino-injected control fish (data not shown). These data indicate that the interaction between PKCε and β-catenin is indispensable for a proper filtration barrier function and depends on several binding sites.

DISCUSSION

We and others have previously shown that the dynamics of the actin cytoskeleton are crucial for podocyte function and often depend on a single player in the network of cytoskeletal signaling components (29). Here we demonstrate that PKCε is a key player in this context via its interaction and regulation of β-catenin (Fig. 6). PKCε dictates the subcellular localization of β-catenin; immunofluorescence staining of PKCε-deficient cells showed that β-catenin translocation from the nucleus to perinuclear areas and membrane during the differentiation depends on PKCε. PKCε shifted β-catenin into the cytosol and to the cellular membrane. Under normal conditions in undifferentiated cells in culture, β-catenin first accumulated in the cytoplasm and was localized to the membrane, while during the differentiation process, excessive β-catenin entered the nucleus to stimulate Wnt target signaling (30).

Use of PMA stimulation as a PKC activator in tissue culture revealed a more detailed picture. PKCε knockout decreased active β-catenin, whereas increasing β-catenin levels were found in control cells. PMA triggers not only PKCε activity (31), but also other C1 domain containing isoforms such as PKCα and PKCβ. PKCα has been previously described as a negative regulator of β-catenin, as its specific inhibition by the small molecule A23187 results in β-catenin upregulation (15), and our data indicate that PKCε might counterbalance the influence of PKCα on β-catenin. We showed that β-catenin and PKCε interact in a GSK3β-independent manner. These results are in line with those of previous studies in other cell types, indicating that PKCα also regulates β-catenin expression separately from GSK3β, when β-catenin is reduced after withdrawing glucose from the medium (32). Our findings also support our previous observation suggesting an antagonistic role of PKCα and PKCβ compared with PKCε in the context of diabetic nephropathy (3). Under physiological conditions β-catenin levels are highly regulated via their phosphorylation sites. The major pathway of β-catenin degradation is via GSK3β, which relies on phosphorylation of β-catenin by CK1 (33). Besides this pathway, alternative pathways of β-catenin degradation are not well characterized. In the Ca2+/DAG dependent pathway, PKCα knockdown leads to an accumulation of β-catenin (16), thus indicating this conventional PKC plays a direct role in β-catenin degradation. In the planar cell polarity pathway, inhibition of PKC δ, another novel PKC, has been shown to induce stabilization of β-catenin (16). Our data define PKCε as an antagonistic regulator of β-catenin stability in both signaling pathways.

PKCε deficient podocytes *in vitro* show a distinct phenotype, displaying an abnormal small cell size, disturbed actin cytoskeleton dynamics, a higher tendency to undergo spontaneous apoptosis and lower expression of podocyte differentiation markers (21). Adenoviral transfection of PKCε -/- podocytes with a PKCε-wildtype construct led to a complete recovery of the cells. Interestingly, a viral transduction of the knockout cells with a human β-catenin construct could also overrule the effects of the PKCε deficiency. The podocytes appeared normal in

size and exhibited a normalized actin cytoskeleton arrangement (Fig. 4A).

P-cadherin, one major factor of the cell-cell adhesion complex of podocytes, was downregulated in PKCε podocytes throughout the differentiation process (Fig. 4C). This finding certainly could explain the poor cell adhesion of PKCε deficient podocytes, since β-catenin and P-cadherin together form a complex and both show a reduced expression. The transfection with PKCε rescued the phenotype as expected. β-Catenin overexpression in PKCε deficient podocytes also induced upregulation of P-cadherin expression, not detected in control transfected cells. This observation surprised us, since it is established that aberrant E-cadherin expression promotes accumulation of an unbound cytoplasmic β-catenin pool. This excessive β-catenin can then further act as a transcription co-factor (34). Our findings suggest that there is rather a mutual relationship between the two proteins, leading to an upregulation of P-cadherin expression by ectopic expression of β-catenin. Further, our results indicate PKCε is a protein that leads to P-cadherin enhancement, rather than downregulation. These results further supplement the described relationship between novel PKCε and P-cadherin, in addition to findings by other groups (35), describing novel PKCs as important regulators of endocytosis and recycling of E-cadherin in other cell types.

Fascin1, a downstream target of the canonical Wnt/β-catenin signaling pathway is an actin filament-bundling protein. It is well known for binding to β-catenin at the cellular edges and possesses a PKC binding site at S39, which has been described for conventional PKCs such as PKCα (24). *Larrson et al.* reported that fascin1 phosphorylation by PKCα leads to a release of fascin1 from the actin bundles, presumably enabling cell spreading (8). However, thus far, an interaction between PKCε and fascin1 has not been presented. Our data suggest an interdependence among PKCε, β-catenin and fascin1, which supports a healthy actin cytoskeleton (Fig.6). Whether the fascin1 upregulation solely relies on increased β-catenin expression mediated per PKCε or could also be induced by PKCε alone needs further investigation, as the rescue of PKCε-/- podocytes with the PKCε construct did not restore fascin1 mRNA expression levels present in wildtype cells, while Western blot analysis suggests a normalized fascin1 protein presence.

The question remains whether the rescue of the PKCε-knockout phenotype by the ß-catenin overexpression is derived from an enhanced Wnt-signaling activity or from accumulation at the cell adhesion complex. We will address this in the future.

We could identify three different PKCε binding/phosphorylation sites in β-catenin, located in its central domain, within the armadillo repeats. This location differs from those for GSK3β and PKCα which have been previously demonstrated to regulate β-catenin via their phosphorylation sites in the N-terminal domain (S33, S37, T41 and S45) (36).

Further studies *in vivo* in the zebrafish model demonstrate that knockdown of β-catenin via morpholino and coinjection of β-catenin RNA lacking S352 or T472/ S473, or S663 cannot rescue the proteinuria phenotype, suggesting these binding sites are indispensable for the phosphorylation of β-catenin by PKCε, leading to its stabilization.

CONCLUSION

In summary, our data indicate that PKCε deficiency leads to low β-catenin expression, defective actin cytoskeleton organization and contributes to disrupted podocyte function leading to an impaired glomerular filtration barrier. Our results further support the hypothesis that balanced β-catenin-levels are important for normal kidney function (12). The novel binding sites of PKCε identified here and its role in β-catenin regulation, opposing those of GSK3β and other PKCs, might represent a new way of counterbalancing physiological β-catenin levels. Therefore our study could be the basis for further pharmacological intervention studies targeting these binding sites, which will be explored in future studies.

EXPERIMENTAL PROCEDURES

Urine analysis

Murine spontaneous spot urine samples were produced by abdomen massage and collected on parafilm. The samples were analyzed by SDS-PAGE and followed by Coomassie Blue staining.

Antibodies and reagents

Primary antibodies used for Western blot, immunoprecipitation and immunofluorescent staining were the following: mouse anti-active-β-catenin (Merck Millipore, Temecula, CA), rabbit anti-β-catenin (Abcam, Cambridge, UK), rabbit anti-phospho-GSK3□/β, rabbit anti-GSK3β, rabbit anti-GFP, rabbit anti-flag (Cell Signaling Technology, Cambridge, UK), rabbit anti-Fascin1 (Abcam, Cambridge, UK), rabbit anti-Paxillin (Merck Millipore, Temecula, CA), goat anti-P-cadherin (Novus Biologicals, Littleton, CO) and rabbit anti-GST (Cell signaling Technology). Secondary antibodies for western blot included the following: goat anti-mouse IgG horseradish peroxidase and goat anti-rabbit IgG horseradish peroxidase, donkey anti-goat IgG horseradish peroxidase, which were all from Santa Cruz Biotechnology (Santa Cruz, CA). The secondary antibody for immunofluorescent staining was mouse Alexa Fluor 488 from Invitrogen (Darmstadt, Germany). Further reagents included Alexa Fluor 546 phalloidin (Invitrogen, Darmstadt, Germany). IP and pulldown assay were performed with FLAG and magnetic GST beads (Sigma-Aldrich, St. Louis, USA).

Western Blot

For protein extractions, podocytes were lysed in radioimmunoprecipitation assay buffer (50 mM Tris pH 7.5, 150 mM NaCl, 0.5% sodium desoxycholate, 1% Nonidet P-40, and 0.1% SDS). The lysates were stored at -80°C overnight and centrifuged at 11,000 rpm for 15 min at 4°C. Afterwards, the supernatant was collected and transferred into a new tube. Protein concentrations were then determined with the BCA (Bicinchoninic Acid) Protein Assay Kit (Thermo Scientific, Rockford, IL, USA) according to the manual. Equal amount of proteins were separated by 10% SDS-PAGE and electro-transferred to the PVDF membrane (Immobilon-P, Millipore, MA, USA). After blocking in 2% BSA (SERVA electrophoresis GmbH, Heidelberg, Germany), the membrane was sequentially probed with the first antibody (1:1000) and HRP-conjugated secondary antibody (1:10,000). The visualization of the HRP signals was achieved with the enhanced chemiluminescence kit (Pierce, Rockford, IL, USA). As loading control either GAPDH or total protein analysis via Coomassie staining of the membrane was used. For the Coomassie staining, the membrane was incubated in 0.1 % Coomassie 250G (w/v) in 50 % (v/v) methanol for 1 minute, destained for 15 minutes in an solution of water/ethanol/acetic acid in the proportion of 4:5:1 and then air-dried overnight.

Cell culture and drug treatment

Cell culture of conditionally immortalized mouse podocytes was performed by following the description of Mundel (37). Under permissive conditions, podocytes proliferation was induced in the presence of 10 U/ml γ-interferon (Cell Sciences, Canton, MA, USA) in the RPMI medium 1640 (Biochrom AG, Berlin, Germany) including 10% FCS and 1% penicillin/streptomycin (both from Gibco Invitrogen GmbH, Karlsruhe, Germany) at 33°C. The podocytes were allowed to differentiate at the nonpermissive temperature of 37°C in the same medium but without γ-interferon. All flasks used for podocytes were coated with collagen-I (BD Biosciences, Bedford, MA, USA), which was mixed in 20 mM sodium acetate (pH 4.7). After being cultured at 37°C for 9 days, the podocytes were pretreated in starvation medium containing 1% of FCS and 1% penicillin/streptomycin for 16 h. On the 10th day of differentiation, the podocytes were treated with PMA (Sigma-Aldrich, St. Louis, USA) and harvested at different time points. For immunocytochemistry, the podocytes were plated on collagen-I coated coverslips in a 24-well plate. To analyze differentiation, podocytes were cultured under nonpermissive conditions and harvested at different timepoints (30 minutes, 1 h, 2 h, 4 h, 8 h, and 24 h).

HEK 293T cells were cultured in DMEM medium (Invitrogen GmbH, Karlsruhe, Germany) containing 10% FCS of and 1% antimycotic solution (Gibco Invitrogen) at 37°C and plated in 10 cm dishes for transfection.

Transfection

HEK 293T cells were seeded in 10-cm dishes two days prior to the transfection. According to the user manual, 1-2 µg plasmid and 6 µl Fugene HD transfection reagent (Promega Corporation, Fitchburg, WI, USA) were mixed gently in 200 µl serum-free medium and incubated for 20 min at room temperature. Afterwards, the mixture was added dropwise into every dish and incubated for 48 h.

Immunoprecipitation

About 48 h after transfection, HEK 293T cells were washed with ice-cold PBS and lysed in 1 ml

ice-cold RIPA buffer (50 mM TrisHCl pH 7.5, 200 mM NaCl, 1 mM EDTA, 1 mM EGTA, 1% Triton-X100, 0.25% Desoxycholic acid sodium salt) with protease inhibitor and phosphatase inhibitor (Roche Diagnostics GmbH, Mannheim, Germany) on ice. The lysate was collected and rotated for 1 h at 4°C and then centrifuged at 11,000 rpm for 15 min at 4°C. The supernatant was transferred into new tubes and 50 µl FLAG beads (Sigma, St. Louis, USA, 50% slurry in Triton buffer) was added to each tube. The tubes were then rotated at 4°C for 3 h. The beads were collected and centrifuged at 3,000 rpm for 3 min, washed with 1ml RIPA buffer and rotated for 5 min at 4°C for 3 times. After detachment from the beads by adding loading buffer and boiling at 95°C, the proteins were separated by SDS-PAGE and analyzed by Western blotting as described above.

Pull-Down assay

30 µl magnetic GST beads (Sigma, St. Louis, USA) were first washed in washing buffer TBS (50 mM Tris Buffered Saline, 138 mM NaCl and 2.7 mM KCl, pH 8.0) before adding either 1 µg of pure recombinant GST or GST-β-catenin (Sigma, St. Louis, USA) protein and rotating the mix for 30 min at room temperature. After washing the mix twice for each 1 minute with 300 µl washing buffer, pure recombinant PKCε protein was added and rotated at 4°C overnight. After washing three times, 120 µl elution buffer (TBS with 15 mM reduced Glutathione, pH 8.0,) was added to the mixture and rotated for 30 minutes. The eluate was then used for separation by SDS-PAGE and analyzed by Western blot.

Immunofluorescence staining

The immortalized mouse podocytes were plated on coverslips for differentiation and fixed with 4 % paraformaldehyde at different time points. After permeabilization with 0.1% Triton X-100, podocytes were blocked in 10 % donkey serum (Jackson Immuno Research, Suffolk, England) for 30 min and incubated with the primary antibody at 4°C overnight and following the incubation of the Alexa-Fluor 488 donkey anti-rabbit IgG and Alexa-Fluor 546 Phalloidin for 1 h (Invitrogen GmbH, Karlsruhe, Germany). Afterwards, glass coverslips were mounted in Aquapolymount medium (Polysciences Inc., Warrington, PA, USA) with DAPI.

For the immunohistochemistry, the murine kidney sections were blocked in 10% donkey serum and incubated with the primary antibody at 4°C overnight. Then the sections were rinsed with TBS for 3 times and incubated with the Alexa-Fluor 488 donkey anti-rabbit IgG for 1 h and mounted with DAPI in Aquapolymount medium. A Zeiss Axioplan-2 imaging microscope and digital image processing software Axio Vision 4.6 (Zeiss, Jena, Germany) were involved for the analysis of the images.

Real-time PCR

Following the manual of the RNeasy Mini Kit (Qiagen, Hilden, Germany), total RNA was extracted from the cultured mouse podocytes. Reverse transcription was performed using 1 µg total RNA, Moloney Murine Leukemia Virus Reverse Transcriptase, Oligo (dT) 15 and random primers (Promega, Mannheim, Germany). The amplification reaction of cDNA was achieved by using Fast Start Taq Polymerase (Roche Diagnostics, Mannheim Germany), SYBR Green (Molecular probes, Eugene, OR) and gene-specific primers in the following thermal cycle: 95°C for 5 min, followed by 45 cycles for 10 s at 95°C, 10 s at 60°C and 10 s at 72°C. Each reaction was performed in triplicate and normalized to the constitutive gene mouse hypoxanthine phosphoribosyl transferase 1 (mHPRT-1). Melting curve analysis was used to verify the specificity of the PCR product. The primers used for amplification were the following: HPRT-1: 5'-CAGTCCCAGCGTCGTGATTA-3', 5'-AGCAAGTCTTTCAGTCCTGTC-3', fascin1: 5'–AACGTGTCCACGCGCC-3', 5'-GCAGCTGGCGTTCTTGGT-3'

Site-directed mutagenesis

After searching in five phosphorylation databases (PhosphoNET, HPRD release 9, dbPTM 3.0, SysPTM 2.0, UniProt), predicted phospho-sites were chosen and compared in five species (human, mouse, zebrafish, Drosophila, and Caenorhabditis elegans) to determine the most conserved ones. Finally, seven promising phospho-motifs were selected as candidates and corresponding site-specific mutations of murine derived DNA were introduced into the plasmid with overlapping PCR. The primers used are listed as follows: S47R forward, 5'-CAGCTCCTTCTCTGAGA(T)GGTAAAGGCA ATCCTG-3'; S47R reverse, 5'-CAGGATTGCCTTTACCT(A)CTCAGAGAAG GAGCTG-3'; S352R forward, 5'-GCTATCTGTCTGCTCTAGA(T)AATAAGCC GGCTATTGTAG-3'; S352R reverse, 5'-

CTACAATAGCCGGCTTATTT(A)CTAGAG CAGACAGATAG- C-3'; T472A and S473R forward, 5'-CTCTTCGTCATCTGG(A)CCAG G(C)CGAC- ACCAAGAAGC-3'; T472A and S473R reverse, 5'-GCTTCTTGGTGTCGC (G)CTGGC(T)CAGATGACGAAGAG-3'; T551A and S552A forward, 5'-CCCAGCGCCGTG(A)CGG(T)CCATGGGTG GG-3'; T551A and S552A reverse, 5'-CCCACCCATGGC(A)CGC(T)ACGGCGCTG GG-3'; S663A forward, 5'-GCTGTTTTGTTCCGAATGG(T)CTGAGGAC AAGCCACAAG-3'; 663A reverse, 5'-CTTGTGGCTTGTCCTCAGC(A)CATTCGGA ACAAAACAGC-3'; S675A forward, 5'-GATTACAAGAAACGGCTTG(T)CAGTTGA GCTGACCAGC-3'; S675A reverse, 5'-GCTGGTCAGCTCAACTGC(A)AAGCCGTTT CTTGTAATC-3'; S715R and S718A forward, 5'-GCCAGGATGATCCTAGG(C)TATCGTG(T)C TTTTCACTCTGGTGG-3'; S715R and S718A reverse, 5'-CCACCAGAGTGAAAAGC(A)ACG ATAC(G)CTAGGATCATCCTGGC-3'.

The original bases were shown in the parentheses. The site-directed mutagenesis was performed with the QuikChange site-directed mutagenesis kit following the instructions recommended by the manufacturer. All constructs were sequenced to verify the nucleotide sequences.

Adenoviral production and infection

Gateway technology (Invitrogen GmbH, Karlsruhe, Germany) was used for the generation of adenoviral vectors. With BP clonase II, donor vectors were established by cloning wildtype or site-directed mutant β-catenin into the pDONR221 vectors. Afterwards adenoviral constructs were generated by recombining pDONR221 with pAd/CMV/V5-DEST, using LR clonase II. All the reactions were accomplished by following the manufacturer's manual. All constructs were confirmed by DNA sequencing. Adenoviral expression and amplification were performed in HEK293 cells. Adenoviral transduction of PKCε -/- podocytes with either pDest, PKCε, or β-catenin constructs was conducted at day 5 of differentiation. About 24 hours later, the medium was changed, and 72 hours post transduction, the cells were harvested or fixed for further analysis.

Cell size

ImageJ was used to quantify the total area of Phalloidin stained podocytes. At least 30 single cells (verified by DAPI staining) of every subgroup were photographed in black and white format.

Zebrafish experiments

We followed the method described by Hentschel (28), zebrafish (L-FABP:DBP-EGFP) were mated and housed at 28.5°C in embryo rearing media (E3). After having been embedded in a 1.2% agarose, the one-cell to four-cell stage fertilized embryos were injected by using Nanoject II injection device (Drummond Scientific, Broomall, PA). For overexpression experiments, mRNA of wildtype or site-directed mutant β-catenin was 1:1 diluted with injection buffer (20 mM HEPES, 200 mM KCl and 0.01% phenol red) and injected at a final concentration of 30 ng/μl in a total volume of 4.6 nl. For rescue experiments, wildtype or site-directed mutant β-catenin mRNA was mixed with β-catenin morpholino, which was diluted in injection buffer, and injected at final concentrations of 30 ng/μl mRNA and 100 μM morpholino in a total volume of 4.6 nl.

Scrambled morpholino was injected as control. Morpholino sequences were designed and ordered from GeneTools (Philomath, OR, USA) as follows: standard control sequence 5'-CCTCTTACCTCAGTTACAATTTATA-3' and β-catenin sequence CTGTGTCAAAAGCTGTATATTCCTG. β-Catenin morpholino sequence was blasted to ensure no off target splice junction or start codon annealing occurred for sequence matches greater than 14nt. At 120 hours post fertilization (hpf) zebrafish larvae were anesthetized with a 1:28 dilution of 4 mg/ml Tricaine (MESAB: ethyl-3aminobenzoate, methanesulfonate acid salt 1% Na2HPO4, pH 7.0) and photographed at 10X magnification. The fluorescence of GFP-labeled vitamin D-binding protein in the pupil of the zebrafish eye was measured and analyzed with ImageJ. The animal protocol was approved by Animal Care and Use Committee of the Mount Desert Island Biological Laboratory (MDIBL), Salisbury Cove, Maine (MDIBL IACUC protocol #14-06).

Statistical analysis

Data are shown as means ± SD and were compared with unpaired Student's *t*-tests; PMA stimulation experiments were compared by using two-way ANOVA analysis. Prism 6 was used for

data analysis. Differences were considered significant at $P < 0.05$.

Ethics statement

Animal work, which was performed following the guidelines of the American Physiologic Society, was approved by Institutional Animal Care and Use Committee of Hannover Medical School and the animal welfare authorities of lower saxony. All efforts were made to minimize the number of animals used and their suffering.

ACKNOWLEDGEMENTS: This work was supported by a grant from the German research council DFG (Schi587/3-6) and BMBF-grant 01GM1518A to MS. Zebrafish experiments were supported by Institutional Development Awards (IDeA) from the National Institute of General Medical Sciences of the National Institutes of Health under grant numbers P20GM0103423 and P20GM104318.

CONFLICT OF INTEREST: The authors declare that they have no conflicts of interest with the content of this article.

AUTHOR CONTRIBUTIONS: MD and XJ and BT conducted all the experiments and analyzed the results. PS was essential with zebrafish experiments. MD and MS wrote the paper, PS and SE were active in editing the manuscript and provided helpful discussions. MS, BT and MD conceived the idea for the project and wrote the paper with MD. All authors reviewed the results and approved the final version of the manuscript.

REFERENCES

1. Mochly-Rosen, D., Das, K., and Grimes, K. V. (2012) Protein kinase C, an elusive therapeutic target? *Nature reviews. Drug discovery* **11**, 937-957
2. Menne, J., Meier, M., Park, J. K., Boehne, M., Kirsch, T., Lindschau, C., Ociepka, R., Leitges, M., Rinta-Valkama, J., Holthofer, H., and Haller, H. (2006) Nephrin loss in experimental diabetic nephropathy is prevented by deletion of protein kinase C alpha signaling in-vivo. *Kidney Int.* **70**, 1456-1462
3. Meier, M., Park, J. K., Overheu, D., Kirsch, T., Lindschau, C., Gueler, F., Leitges, M., Menne, J., and Haller, H. (2007) Deletion of protein kinase C-beta isoform in vivo reduces renal hypertrophy but not albuminuria in the streptozotocin-induced diabetic mouse model. *Diabetes* **56**, 346-354
4. Meier, M., Menne, J., Park, J. K., Holtz, M., Gueler, F., Kirsch, T., Schiffer, M., Mengel, M., Lindschau, C., Leitges, M., and Haller, H. (2007) Deletion of protein kinase C-epsilon signaling pathway induces glomerulosclerosis and tubulointerstitial fibrosis in vivo. *J. Am. Soc. Nephrol.* **18**, 1190-1198
5. Teng, B., Duong, M., Tossidou, I., Yu, X., and Schiffer, M. (2014) Role of protein kinase C in podocytes and development of glomerular damage in diabetic nephropathy. *Front. Endocrinol. (Lausanne)* **5**, 179
6. Inagaki, K., Churchill, E., and Mochly-Rosen, D. (2006) Epsilon protein kinase C as a potential therapeutic target for the ischemic heart. *Cardiovasc. Res.* **70**, 222-230
7. Obis, T., Besalduch, N., Hurtado, E., Nadal, L., Santafe, M. M., Garcia, N., Tomas, M., Priego, M., Lanuza, M. A., and Tomas, J. (2015) The novel protein kinase C epsilon isoform at the adult neuromuscular synapse: location, regulation by synaptic activity-dependent muscle contraction through TrkB signaling and coupling to ACh release. *Mol. Brain* **8**, 8
8. Larsson, C. (2006) Protein kinase C and the regulation of the actin cytoskeleton. *Cell. Signal.* **18**, 276-284
9. Prekeris, R., Mayhew, M. W., Cooper, J. B., and Terrian, D. M. (1996) Identification and localization of an actin-binding motif that is unique to the epsilon isoform of protein kinase C and participates in the regulation of synaptic function. *J. Cell Biol.* **132**, 77-90

10. Voronkov, A., and Krauss, S. (2013) Wnt/beta-catenin signaling and small molecule inhibitors. *Curr. Pharm. Des.* **19**, 634-664
11. Dai, C., Stolz, D. B., Kiss, L. P., Monga, S. P., Holzman, L. B., and Liu, Y. (2009) Wnt/beta-catenin signaling promotes podocyte dysfunction and albuminuria. *J. Am. Soc. Nephrol.* **20**, 1997-2008
12. Kato, H., Gruenwald, A., Suh, J. H., Miner, J. H., Barisoni-Thomas, L., Taketo, M. M., Faul, C., Millar, S. E., Holzman, L. B., and Susztak, K. (2011) Wnt/beta-catenin pathway in podocytes integrates cell adhesion, differentiation, and survival. *J. Biol. Chem.* **286**, 26003-26015
13. Willert, K., and Nusse, R. (1998) Beta-catenin: a key mediator of Wnt signaling. *Curr. Opin. Genet. Dev.* **8**, 95-102
14. Sheldahl, L. C., Park, M., Malbon, C. C., and Moon, R. T. (1999) Protein kinase C is differentially stimulated by Wnt and Frizzled homologs in a G-protein-dependent manner. *Curr. Biol.* **9**, 695-698
15. Gwak, J., Cho, M., Gong, S. J., Won, J., Kim, D. E., Kim, E. Y., Lee, S. S., Kim, M., Kim, T. K., Shin, J. G., and Oh, S. (2006) Protein-kinase-C-mediated beta-catenin phosphorylation negatively regulates the Wnt/beta-catenin pathway. *J. Cell Sci.* **119**, 4702-4709
16. Hernandez-Maqueda, J. G., Luna-Ulloa, L. B., Santoyo-Ramos, P., Castaneda-Patlan, M. C., and Robles-Flores, M. (2013) Protein kinase C delta negatively modulates canonical Wnt pathway and cell proliferation in colon tumor cell lines. *PLoS One* **8**, e58540
17. Gwak, J., Jung, S. J., Kang, D. I., Kim, E. Y., Kim, D. E., Chung, Y. H., Shin, J. G., and Oh, S. (2009) Stimulation of protein kinase C-alpha suppresses colon cancer cell proliferation by down-regulation of beta-catenin. *J. Cell. Mol. Med.* **13**, 2171-2180
18. Davidson, K. C., Adams, A. M., Goodson, J. M., McDonald, C. E., Potter, J. C., Berndt, J. D., Biechele, T. L., Taylor, R. J., and Moon, R. T. (2012) Wnt/beta-catenin signaling promotes differentiation, not self-renewal, of human embryonic stem cells and is repressed by Oct4. *Proc. Natl. Acad. Sci. U. S. A.* **109**, 4485-4490
19. Otero, J. J., Fu, W., Kan, L., Cuadra, A. E., and Kessler, J. A. (2004) β-Catenin signaling is required for neural differentiation of embryonic stem cells. *Development* **131**, 3545-3557
20. Fang, X., Yu, S. X., Lu, Y., Bast, R. C., Jr., Woodgett, J. R., and Mills, G. B. (2000) Phosphorylation and inactivation of glycogen synthase kinase 3 by protein kinase A. *Proc. Natl. Acad. Sci. U. S. A.* **97**, 11960-11965
21. Schiffer, M., Teng, B., Gu, C., Shchedrina, V. A., Kasaikina, M., Pham, V. A., Hanke, N., Rong, S., Gueler, F., Schroder, P., Tossidou, I., Park, J. K., Staggs, L., Haller, H., Erschow, S., Hilfiker-Kleiner, D., Wei, C., Chen, C., Tardi, N., Hakroush, S., Selig, M. K., Vasilyev, A., Merscher, S., Reiser, J., and Sever, S. (2015) Pharmacological targeting of actin-dependent dynamin oligomerization ameliorates chronic kidney disease in diverse animal models. *Nat. Med.* **21**, 601-609
22. Reiser, J., Kriz, W., Kretzler, M., and Mundel, P. (2000) The glomerular slit diaphragm is a modified adherens junction. *J. Am. Soc. Nephrol.* **11**, 1-8
23. Jayo, A., and Parsons, M. (2010) Fascin: a key regulator of cytoskeletal dynamics. *Int. J. Biochem. Cell Biol.* **42**, 1614-1617
24. Anilkumar, N., Parsons, M., Monk, R., Ng, T., and Adams, J. C. (2003) Interaction of fascin and protein kinase Calpha: a novel intersection in cell adhesion and motility. *EMBO J.* **22**, 5390-5402
25. Li, A., Dawson, J. C., Forero-Vargas, M., Spence, H. J., Yu, X., Konig, I., Anderson, K., and Machesky, L. M. (2010) The actin-bundling protein fascin stabilizes actin in invadopodia and potentiates protrusive invasion. *Curr. Biol.* **20**, 339-345
26. Bellipanni, G., Varga, M., Maegawa, S., Imai, Y., Kelly, C., Myers, A. P., Chu, F., Talbot, W. S., and Weinberg, E. S. (2006) Essential and opposing roles of zebrafish beta-catenins in the formation of dorsal axial structures and neurectoderm. *Development* **133**, 1299-1309
27. Hao, J., Ao, A., Zhou, L., Murphy, C. K., Frist, A. Y., Keel, J. J., Thorne, C. A., Kim, K., Lee, E., and Hong, C. C. (2013) Selective small molecule targeting beta-catenin function discovered by in vivo chemical genetic screen. *Cell reports* **4**, 898-904

28. Hentschel, D. M., Mengel, M., Boehme, L., Liebsch, F., Albertin, C., Bonventre, J. V., Haller, H., and Schiffer, M. (2007) Rapid screening of glomerular slit diaphragm integrity in larval zebrafish. *Am. J. Physiol. Renal Physiol.* **293**, F1746-1750
29. Perico, L., Conti, S., Benigni, A., and Remuzzi, G. (2016) Podocyte-actin dynamics in health and disease. *Nature reviews. Nephrology* **12**, 692-710
30. Behrens, J. (2005) The role of the Wnt signalling pathway in colorectal tumorigenesis. *Biochem. Soc. Trans.* **33**, 672-675
31. Newton, P. M., and Messing, R. O. (2010) The substrates and binding partners of protein kinase Cepsilon. *Biochem. J.* **427**, 189-196
32. Choi, S. W., Song, J. K., Yim, Y. S., Yun, H. G., and Chun, K. H. (2015) Glucose deprivation triggers protein kinase C-dependent beta-catenin proteasomal degradation. *J. Biol. Chem.* **290**, 9863-9873
33. Luna-Ulloa, L. B., Hernandez-Maqueda, J. G., Castaneda-Patlan, M. C., and Robles-Flores, M. (2011) Protein kinase C in Wnt signaling: implications in cancer initiation and progression. *IUBMB Life* **63**, 915-921
34. Orsulic, S., Huber, O., Aberle, H., Arnold, S., and Kemler, R. (1999) E-cadherin binding prevents beta-catenin nuclear localization and beta-catenin/LEF-1-mediated transactivation. *J. Cell Sci.* **112 (Pt 8)**, 1237-1245
35. Le, T. L., Joseph, S. R., Yap, A. S., and Stow, J. L. (2002) Protein kinase C regulates endocytosis and recycling of E-cadherin. *Am. J. Physiol. Cell Physiol.* **283**, C489-499
36. Liu, C., Li, Y., Semenov, M., Han, C., Baeg, G. H., Tan, Y., Zhang, Z., Lin, X., and He, X. (2002) Control of beta-catenin phosphorylation/degradation by a dual-kinase mechanism. *Cell* **108**, 837-847
37. Mundel, P., Reiser, J., and Kriz, W. (1997) Induction of differentiation in cultured rat and human podocytes. *J. Am. Soc. Nephrol.* **8**, 697-705

FIGURE LEGEND

Figure 1. ***β-catenin expression in glomeruli of wildtype and PKCε-knockout mice***. A) Immunofluorescence staining of murine glomeruli at 12 weeks of age in PKCε +/+ and PKCε -/- mice. Costaining with β-catenin (green), podocyte marker synaptopodin (red), and DAPI (blue) show expression and localization within glomeruli. B) Semiquantitative analysis of the number of cells with β-catenin expression in PKCε +/+ and PKCε -/- mice (****$p < 0.0001$). C) SDS-PAGE/Coomassie gel staining of urine from wildtype and PKCε -knockout mice at 9 and 12 weeks. BSA at 1, 5, and 10 µg/mL served both as a control and standard. Data are mean ± SD of at least three different independent experiments.

Figure 2. ***PKCε influences subcellular β-catenin expression and activity.*** A) Western blot analysis of active β-catenin expression in murine podocytes from day 0 and day 10. B) Immunofluorescent staining of PKCε +/+ and PKCε -/- podocytes at different time points of differentiation (d0, d4, and d8) show the subcellular localization of β-Catenin (green). Phalloidin staining labels the actin cytoskeleton (red). White arrows indicate membrane localization of β-catenin at cell-cell contacts. Scale bar = 40 µm. C) Ratio of nuclear to perinuclear β-catenin was determined by measuring the mean fluorescence intensity with ImageJ. Graph shows the ratio of nuclear to perinuclear β-catenin fluorescence intensity, displaying the reversed shift of subcellular localization of β-catenin during the differentiation (* $p < 0.05$, ** $p < 0.05$, *** $p < 0.0001$ by Student's t-test). Data are represented as mean ± SD of at least three different independent experiments.

Figure 3. ***PKCε stabilized β-catenin independently from GSK3β.*** A) Differentiated PKCε +/+ and PKCε -/- podocytes were treated with PMA for 0.5, 1, 2, 4, 8, and 12 hours and then harvested for Western blot analysis. Untreated cells (0 hours) served as a control. B) Active β-catenin expression was normalized to GAPDH. Two-way ANOVA analysis of active β-catenin expression of PKCε +/+ and PKCε -/- cells under PMA stimulation at 1, 2, 4, 8, and 24 hrs was performed. C) PKCε +/+ and PKCε -/- podocytes were treated as in A) and analyzed for GSK3β and p-GSK3 α /β expression. D) GSK3β protein level was normalized to GAPDH. Data represent mean ± SEM of three different independent experiments in B and D.

Figure 4. ***Overexpression of β-catenin rescues phenotype of PKCε knockout podocytes.*** A) Murine PKCε -/- podocytes were transduced with adenoviral vectors expressing either pAd-Dest, PKCε, or β-catenin. Immunofluorescence staining of the actin cytoskeleton with phalloidin and against paxillin. B) Cell size of the phalloidin-marked podocytes was assessed in ImageJ for the determination of the mean area. C) Western blot analysis of P-cadherin expression in murine podocytes from day 0 and day 10. D) PKCε -/- podocytes were transduced with adenoviral vectors expressing either pAd-Dest, PKCε or β-catenin and then analyzed for P-cadherin expression with Western blot. E) Quantification of the P-cadherin band intensity using total protein analysis with coomassie staining of the membrane. F) qRT-PCR of RNA extracted from cells of the same experiment as in A) was used to assess the fascin1 mRNA expression and normalized to HPRT. G) Western blot analysis of the same experiment as in A) for fascin1 protein expression. H) Quantification of the band intensity by total protein analysis with Coomassie staining (* $p < 0.05$, ** $p < 0.05$, *** $p < 0.0001$ by Student's t-test). Data are represented as mean ± SD of at least three different independent experiments.

Figure 5. ***PKCε is a functional binding partner of β-catenin and the interaction is indispensable for filtration barrier function.*** A) FLAG immunoprecipitation of HEK cells transduced with a FLAG-tagged β-catenin construct and either a GFP, GFP-tagged PKCα (positive control) or GFP-tagged PKCε construct. Immunoblotting against FLAG shows a successful transfection. B) In vitro direct interaction between β-catenin and PKCε was examined in a GST pulldown experiment with pure recombinant GST-β-catenin and His-PKCε. His-PKCε was incubated with either GST or GST-β-catenin. The pulldown fractions were analyzed by western immunoblotting against PKCε and GST. C) Schematic diagram illustrating β-catenin protein structure, which is divided into the N-terminal, the Armadillo-repeats and the C-terminal part. The suggested phosphorylation sites of PKCε are shown. D) The pictures show individual larvae at 120 hours post fertilization (hpf), indicating control morpholino injected fish with no edema and β-catenin morpholino injected fish with edema and a dorsolized phenotype. E) The murine β-catenin-mutants were tested in the zebrafish model by injecting the capped-mRNA into fertilized zebrafish eggs at one-to-four cell stage embryos. The transgenic zebrafish produce a vitamin D-binding protein fused with GFP, which under normal conditions accumulates in the retina and is quantified 120 hpf by measuring the fluorescence level. Reduced fluorescence indicates a disturbed glomerular filtration barrier. The graph shows GFP fluorescence intensity of the eye assay of wildtype, β-catenin1 morpholino, and co-injection of β-catenin1 morpholino with a human wildtype RNA construct. F) The graph shows group mean fluorescence intensities of the eye assay. Comparison of the combined injection of β-catenin morpholino plus β-catenin-mutant results was conducted against β-catenin morpholino injection alone (* $p < 0.05$, ** $p < 0.01$, *** $p < 0.001$). Binding of each β-catenin mutant to GFP-tagged PKCε was tested *in vitro* with FLAG immunoprecipitation in transfected HEK cells. Immunoblotting was performed against GFP and FLAG.

Figure 6. ***Schematic overview of β-catenin regulation by PKCε in wildtype and PKCε -/- podocytes.*** In wildtype podocytes, PKCε regulates cytoplasmic β-catenin level in balance with other PKC isoforms: PKCα phosphorylates β-catenin and thus leads to its degradation. PKCε inhibits the degradation via its

interaction sites (S352, T472/S473 and S663) in a GSK3β independent manner and leads to a predominantly cytosolic localization of β-catenin, which then might bind to the actin-bundling protein fascin1 in filopodia of the podocytes or localize to the membrane forming the cell adhesion complex with P-cadherin and α-catenin, resulting in a stabilized actin cytoskeleton and cell adhesion. In PKCε-deficient podocytes this balance is disturbed, leading to the degradation of β-catenin, abolished p-cadherin expression and lower fascin1 expression which then results in impaired cell adhesion and actin bundling and thus in a weakened actin cytoskeleton.

Figure 1

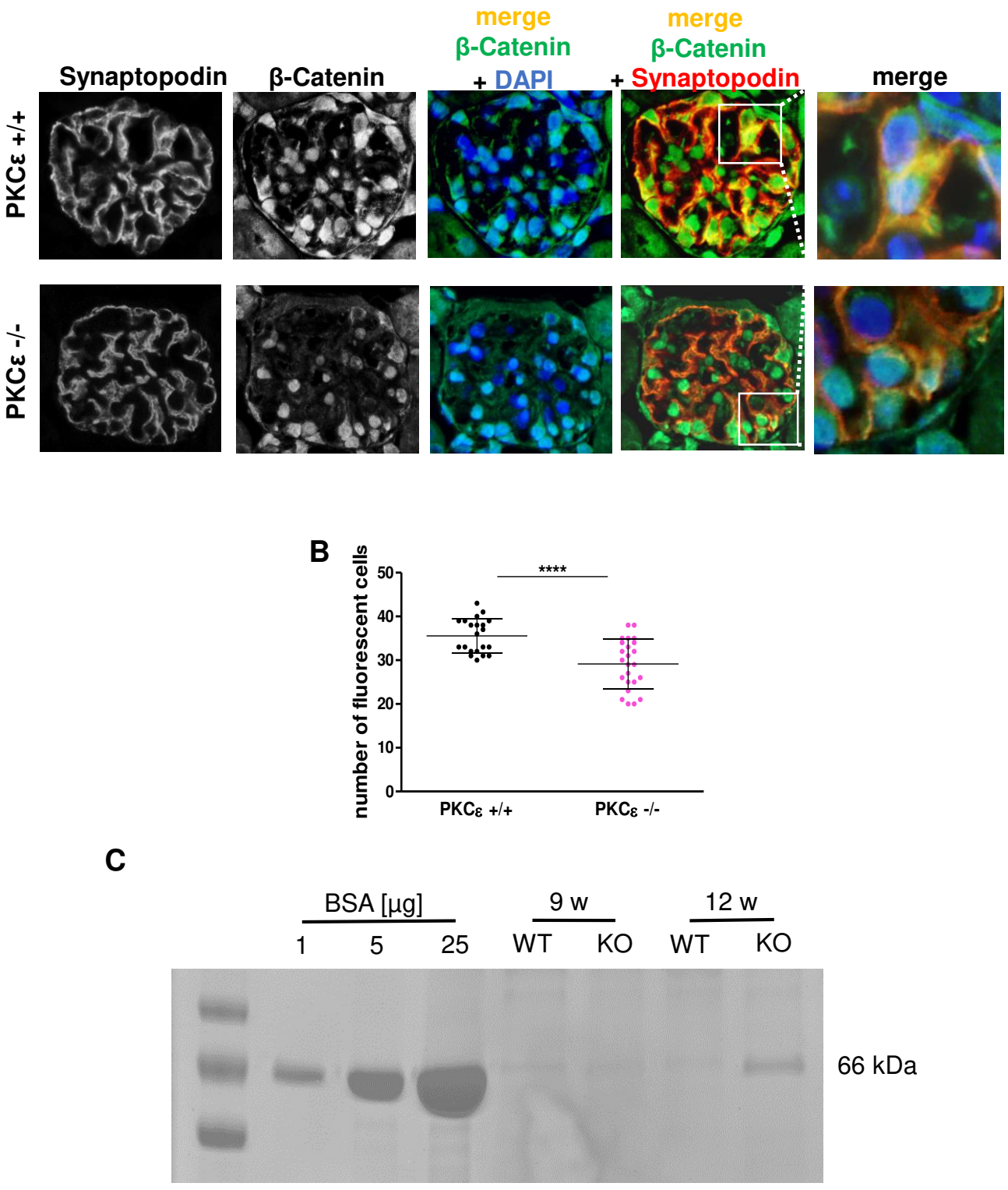
A
Synaptopodin
β-Catenin
merge
β-Catenin
+ DAPI
merge
β-Catenin
+ Synaptopodin
merge
PKCε +/+
PKCε -/-
B
number of fluorescent cells
****
50
40
30
20
10
0
PKCε +/+
PKCε -/-
C
BSA [µg]
1
5
25
9 w
WT
KO
12 w
WT
KO
66 kDa

Figure 2

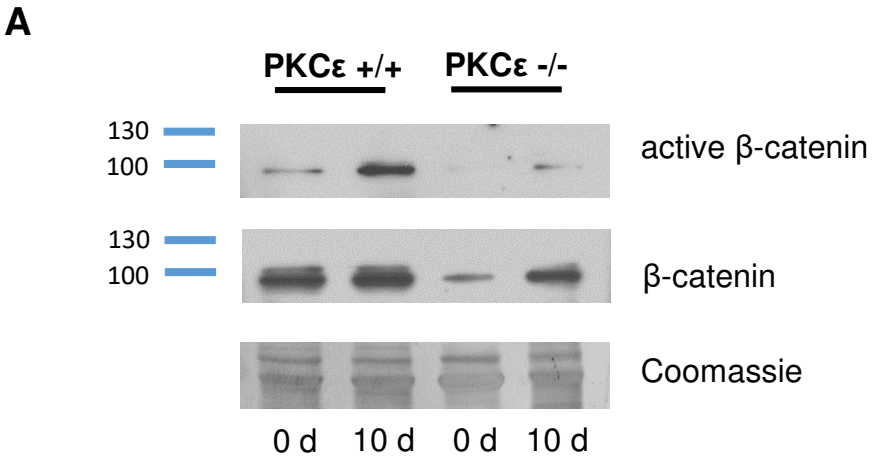
A
PKCε +/+
PKCε -/-
130
100
active β-catenin
130
100
β-catenin
Coomassie
0 d
10 d
0 d
10 d

Figure 2

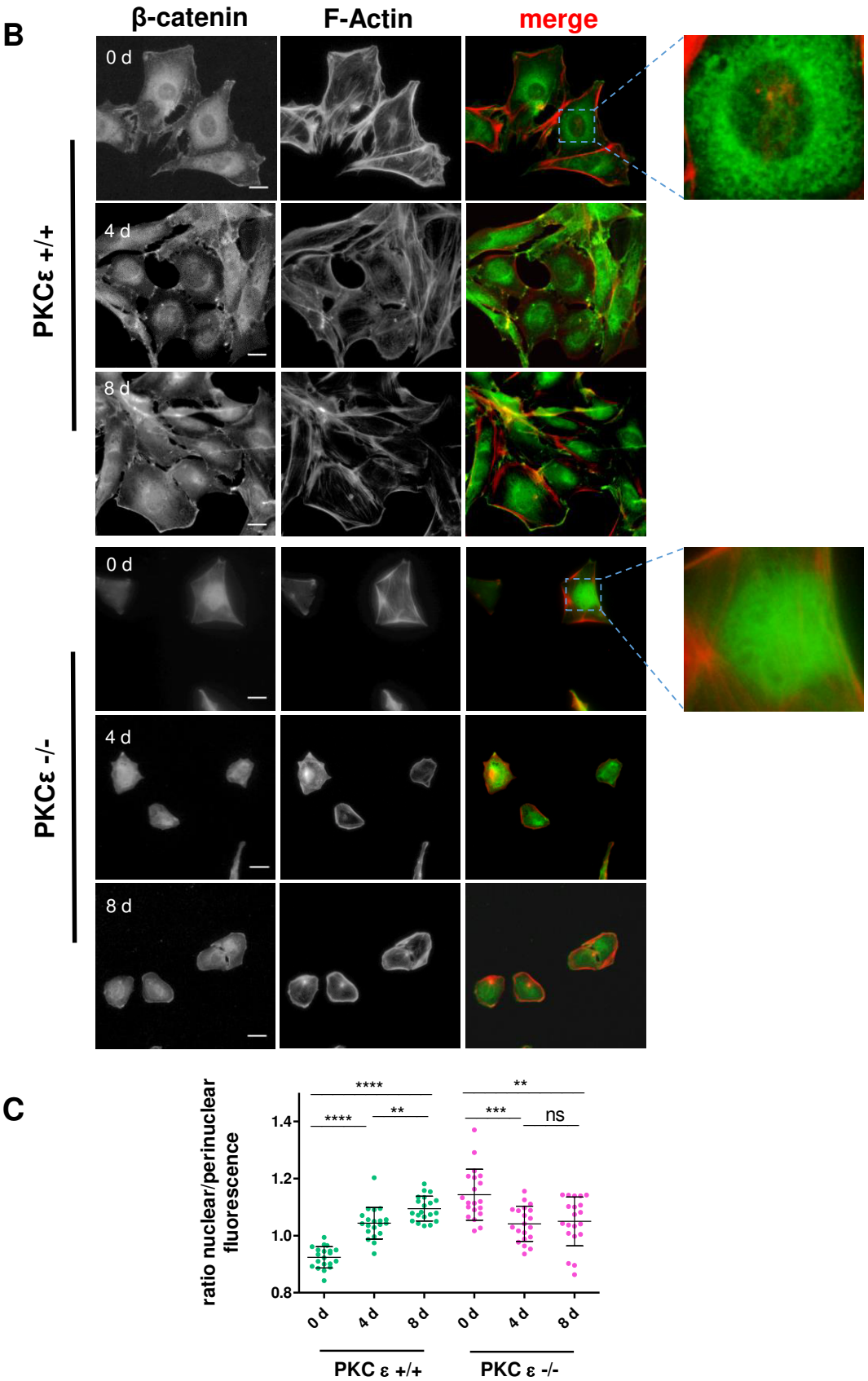
B
β-catenin
F-Actin
merge
0 d
4 d
8 d
PKCε +/+
PKCε -/-
C
ratio nuclear/perinuclear fluorescence
1.4
1.2
1.0
0.8
****
**
****
**
***
ns
0 d
4 d
8 d
0 d
4 d
8 d
PKC ε +/+
PKC ε -/-

Figure 3

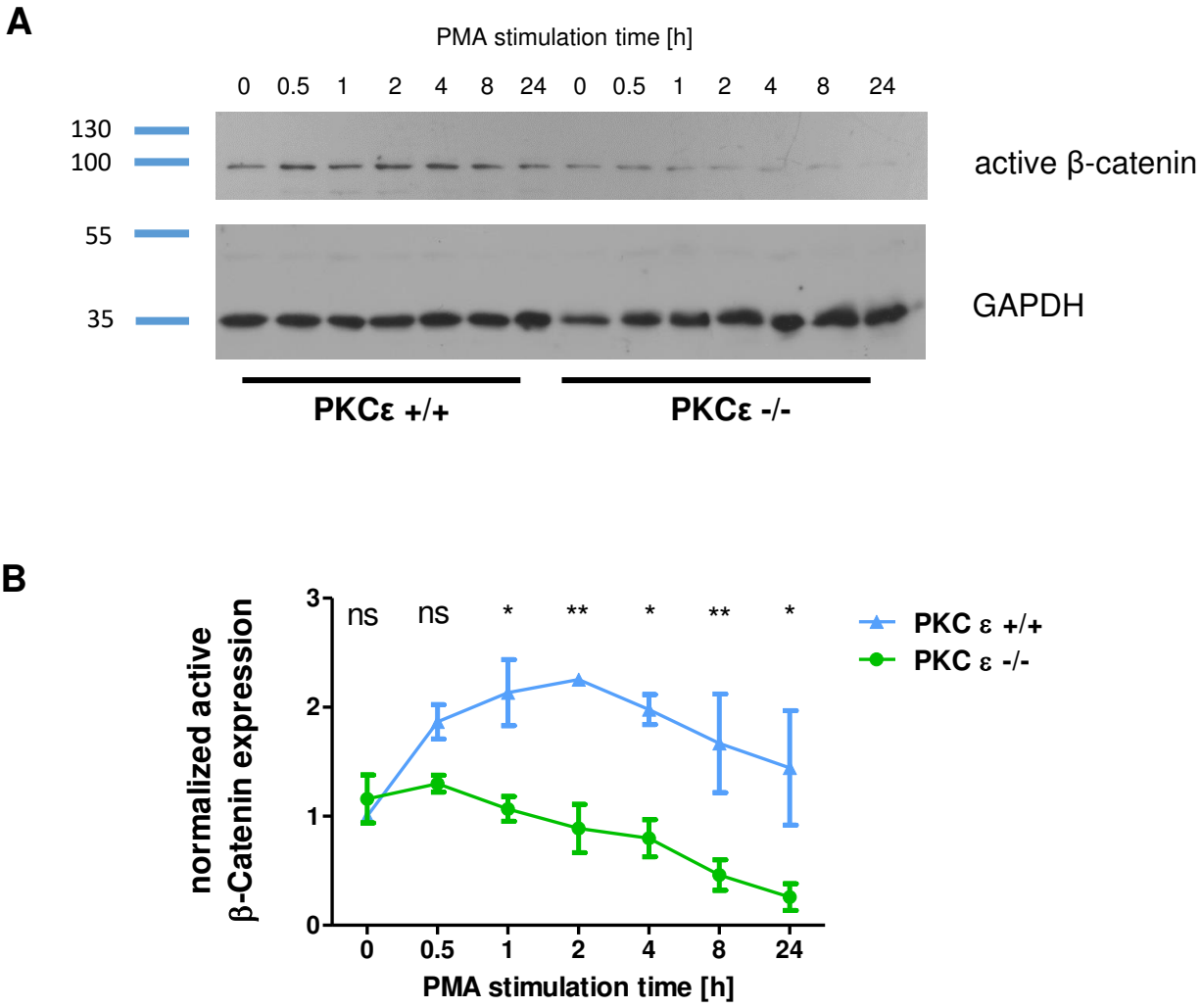
A
PMA stimulation time [h]
0 0.5 1 2 4 8 24 0 0.5 1 2 4 8 24
130
100
55
35
active β-catenin
GAPDH
PKCε +/+
PKCε -/-
B
normalized active β-Catenin expression
ns ns * ** * ** *
PKC ε +/+
PKC ε -/-
0 0.5 1 2 4 8 24
PMA stimulation time [h]

Figure 3

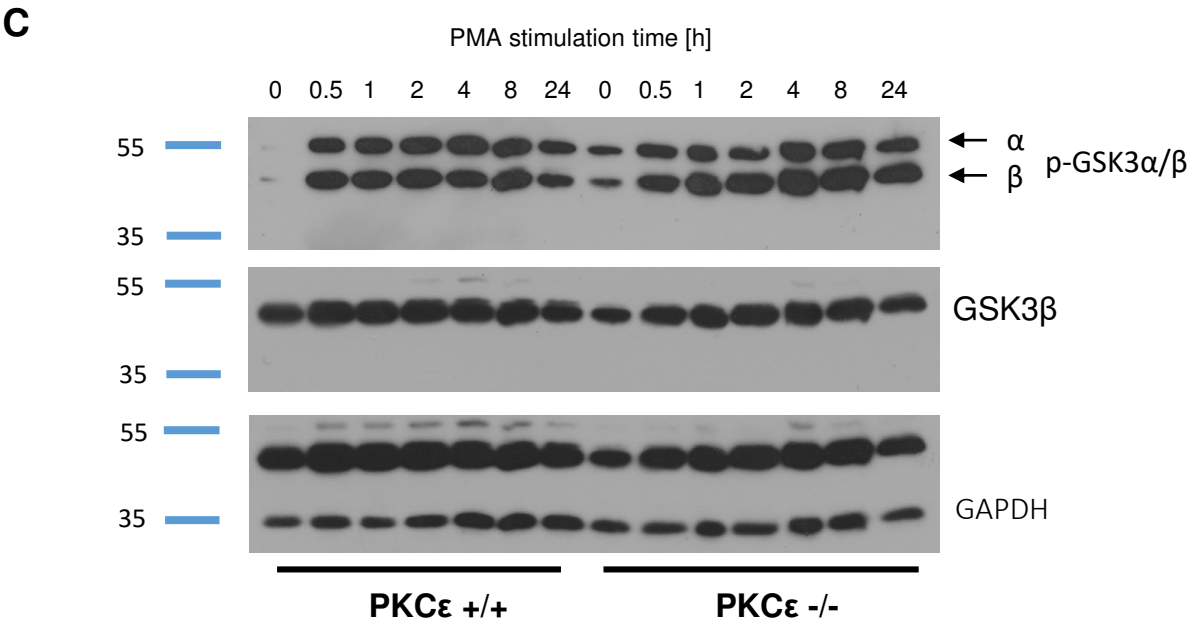
C
PMA stimulation time [h]
0 0.5 1 2 4 8 24 0 0.5 1 2 4 8 24
55
35
55
35
55
35
α
β
p-GSK3α/β
GSK3β
GAPDH
PKCε +/+
PKCε -/-

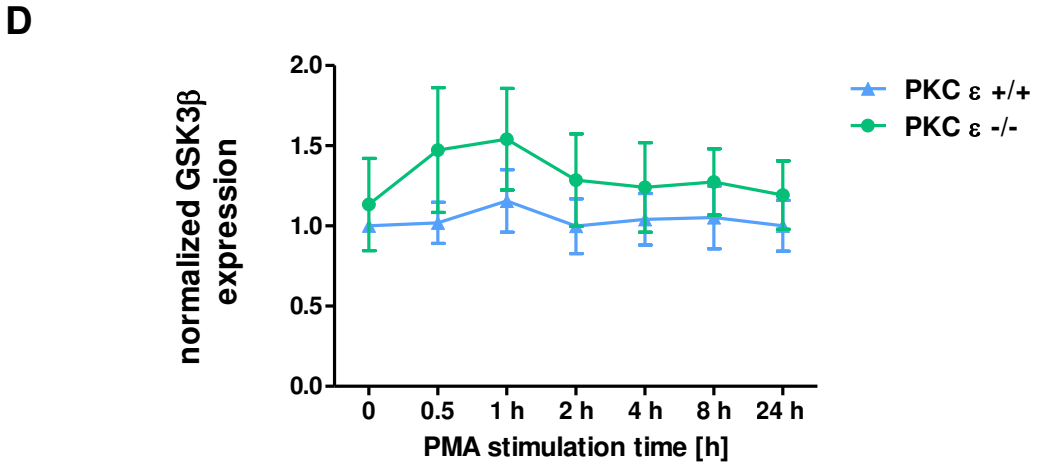
D
normalized GSK3β expression
2.0
1.5
1.0
0.5
0.0
0
0.5
1 h
2 h
4 h
8 h
24 h
PMA stimulation time [h]
PKC ε +/+
PKC ε -/-

Figure 4

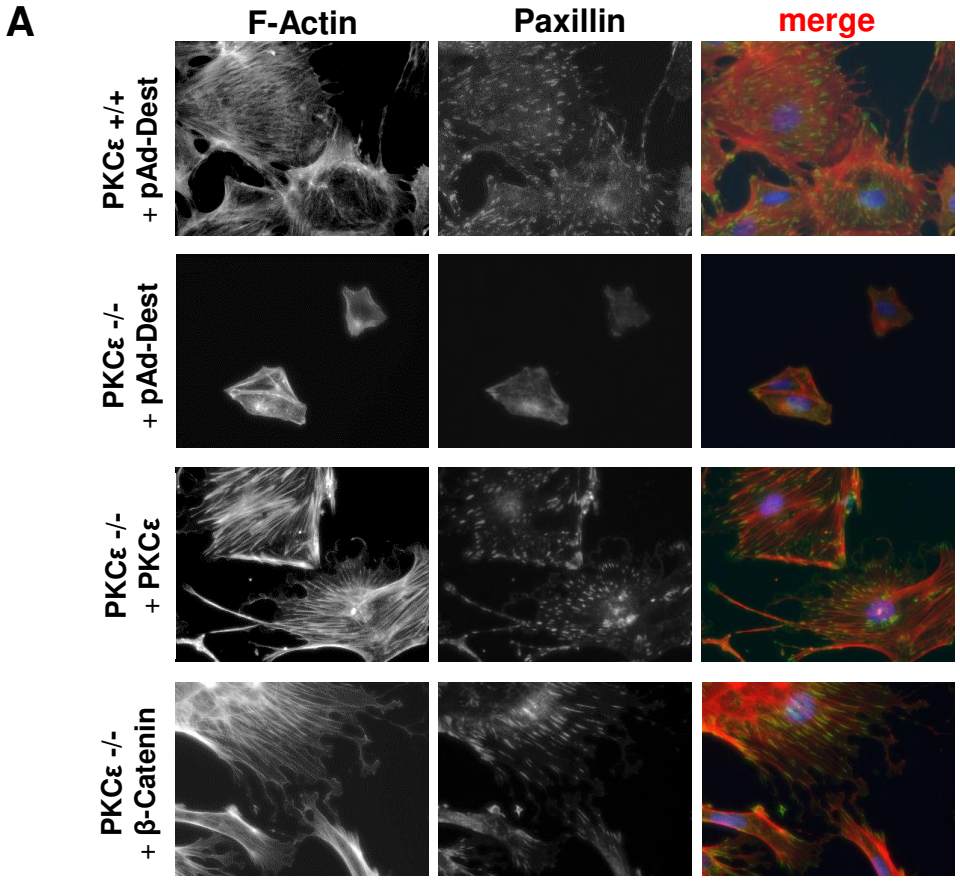
A
F-Actin
Paxillin
merge
PKCε +/+
+ pAd-Dest
PKCε -/-
+ pAd-Dest
PKCε -/-
+ PKCε
PKCε -/-
+ β-Catenin

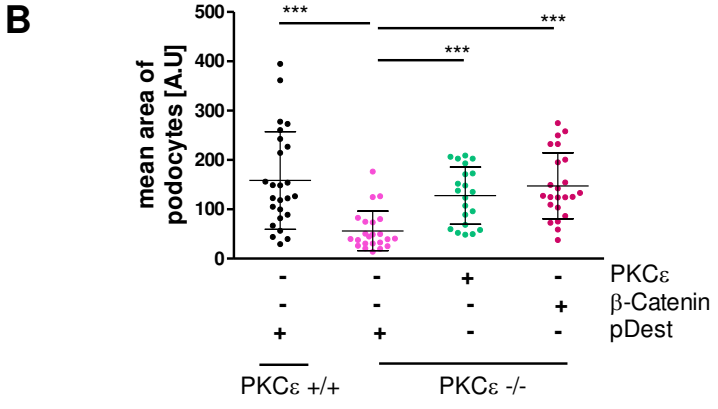
B
mean area of podocytes [A.U]
500
400
300
200
100
0
***
***
***
PKCε
β-Catenin
pDest
PKCε +/+
PKCε -/-

Figure 4

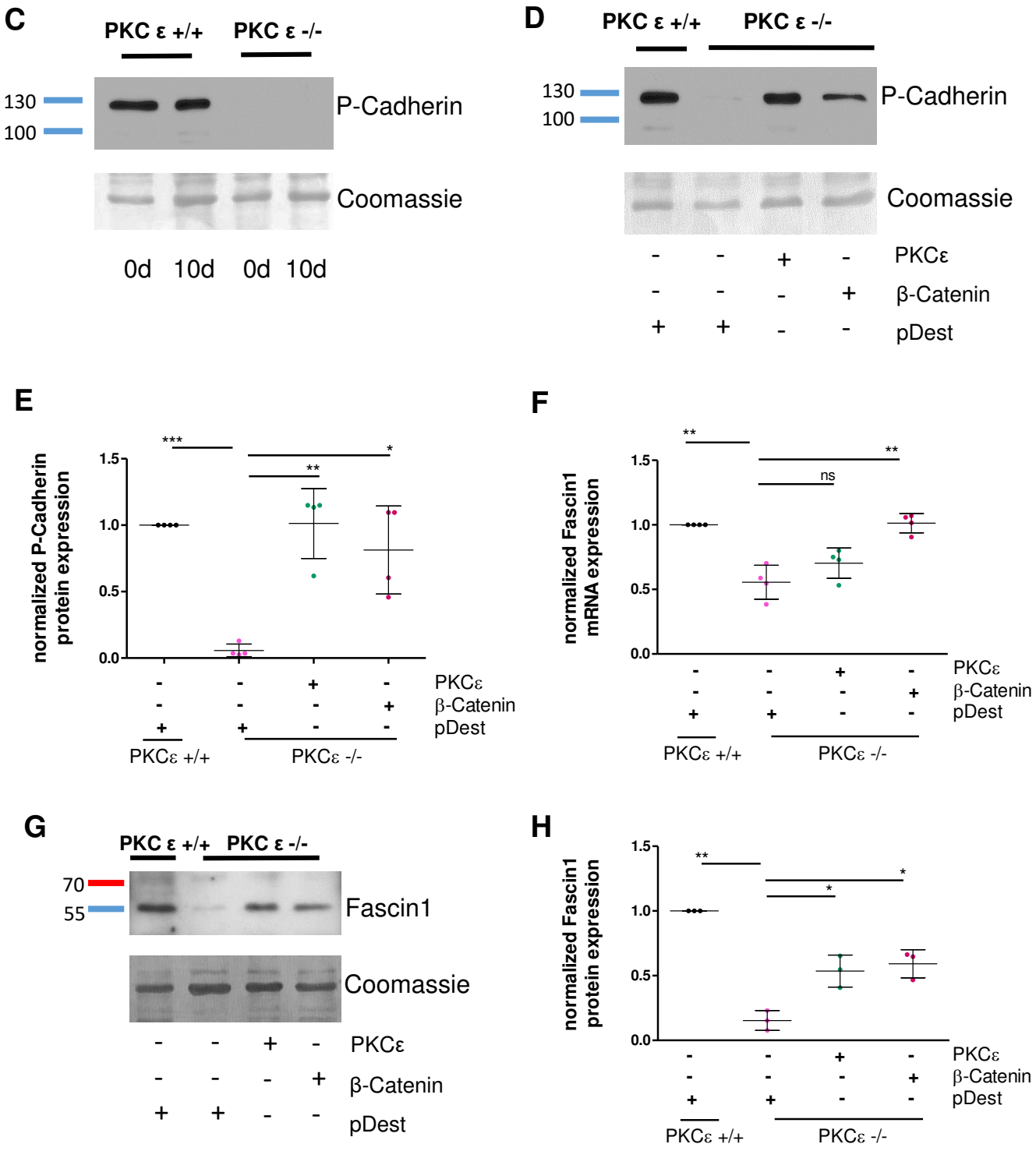
C
PKC ε +/+
PKC ε -/-
130
100
P-Cadherin
Coomassie
0d 10d 0d 10d
D
PKC ε +/+
PKC ε -/-
130
100
P-Cadherin
Coomassie
PKCε
β-Catenin
pDest
E
normalized P-Cadherin protein expression
PKCε
β-Catenin
pDest
PKCε +/+
PKCε -/-
F
normalized Fascin1 mRNA expression
ns
PKCε
β-Catenin
pDest
PKCε +/+
PKCε -/-
G
PKC ε +/+
PKC ε -/-
70
55
Fascin1
Coomassie
PKCε
β-Catenin
pDest
H
normalized Fascin1 protein expression
PKCε
β-Catenin
pDest
PKCε +/+
PKCε -/-

Figure 5

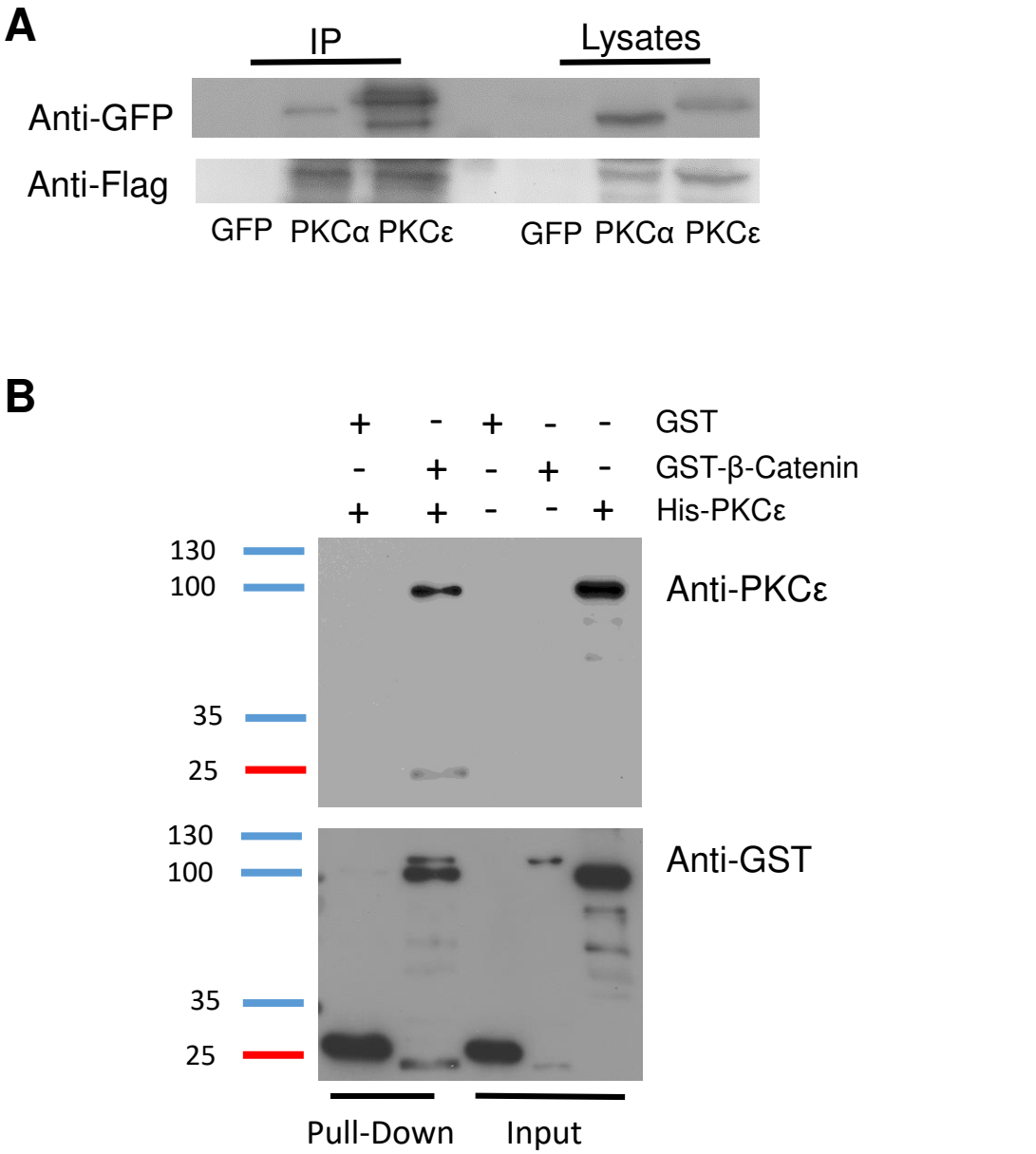
A
IP
Lysates
Anti-GFP
Anti-Flag
GFP PKCα PKCε
GFP PKCα PKCε
B
+ - + - - GST
- + - + - GST-β-Catenin
+ + - - + His-PKCε
130
100
35
25
Anti-PKCε
130
100
35
25
Anti-GST
Pull-Down
Input
C
S47R
S352R
T472A/S473R
T551A/S552A
S663A
S675A
S715R/S718A
NH2
COOH
1
141
664
781
armadillo repeats

Figure 5

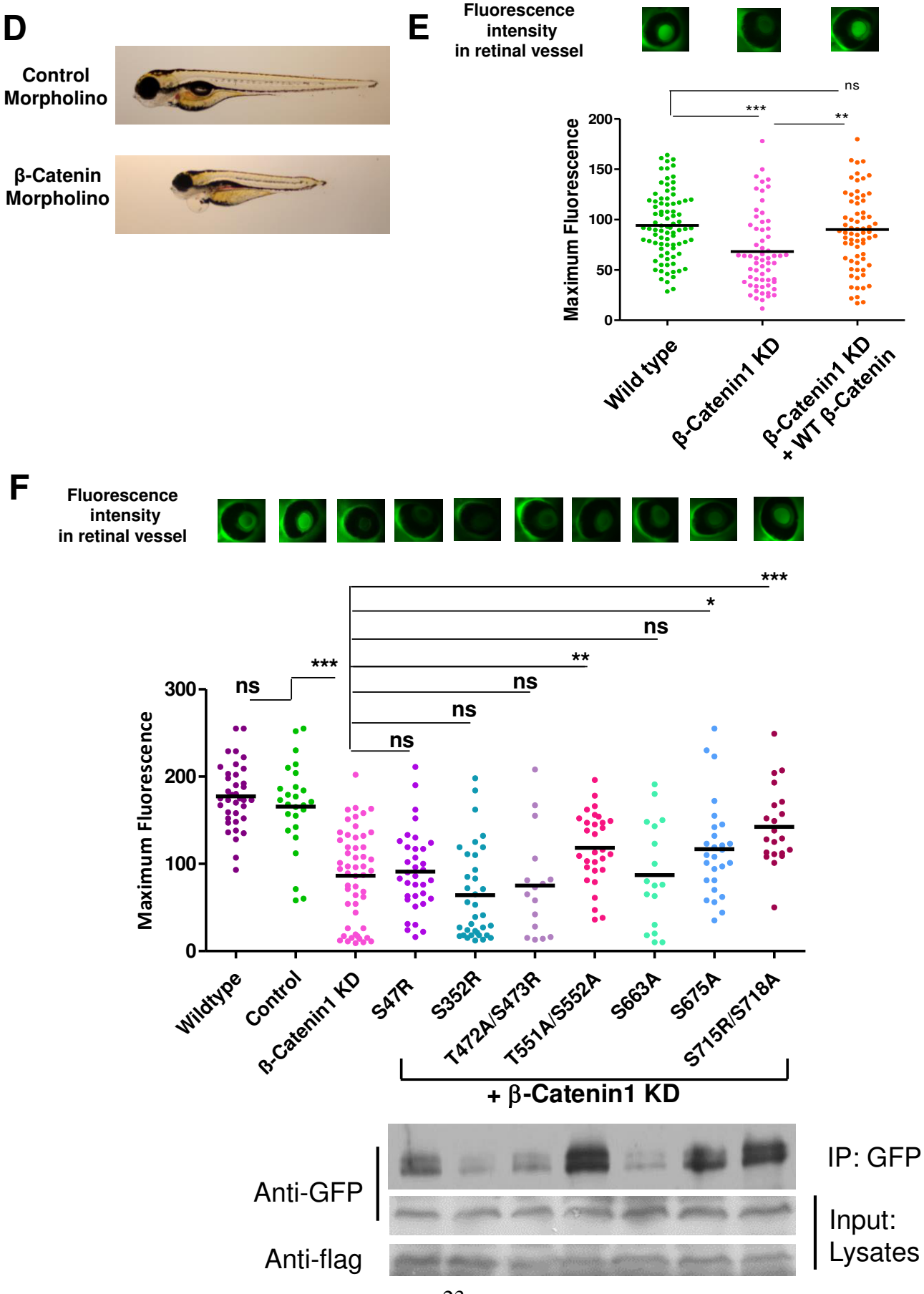
D
Control Morpholino
β-Catenin Morpholino
E
Fluorescence intensity in retinal vessel
Maximum Fluorescence
ns
***
**
Wild type
β-Catenin1 KD
β-Catenin1 KD + WT β-Catenin
F
Fluorescence intensity in retinal vessel
Maximum Fluorescence
Wildtype
Control
β-Catenin1 KD
S47R
S352R
T472A/S473R
T551A/S552A
S663A
S675A
S715R/S718A
+ β-Catenin1 KD
Anti-GFP
Anti-flag
IP: GFP
Input: Lysates

Figure 6

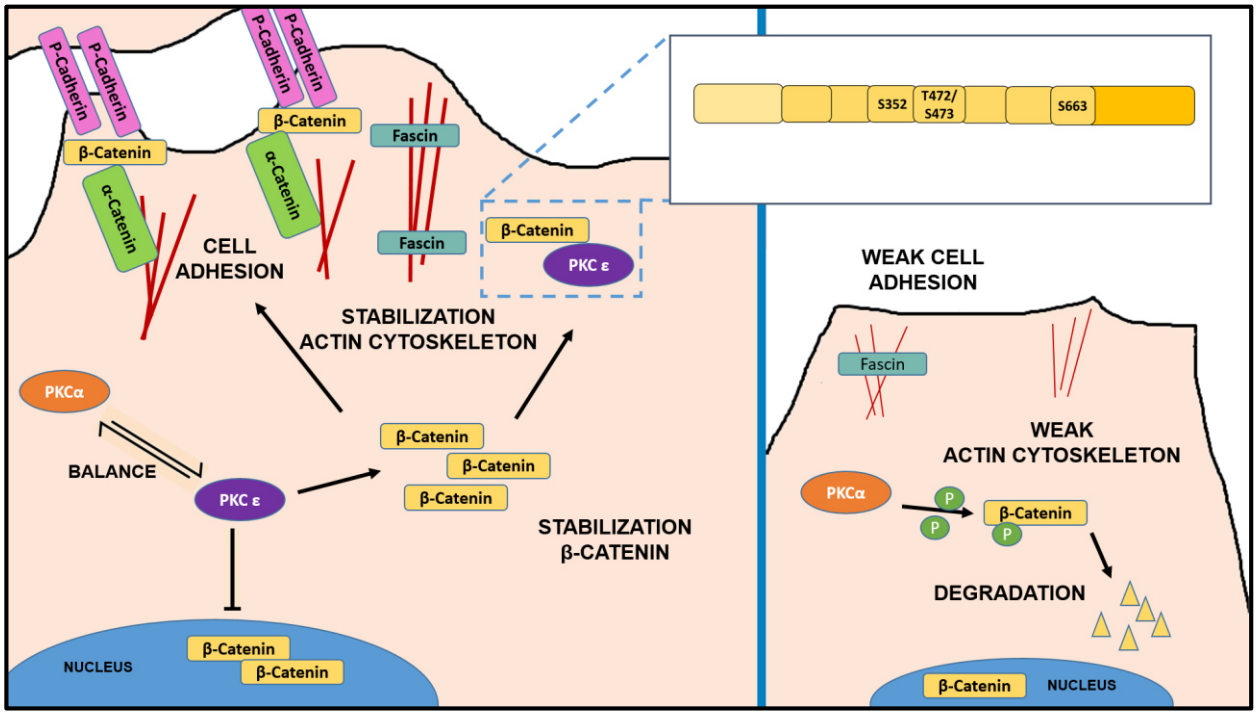

WILD TYPE PODOCYTES

PKCε KNOCKOUT PODOCYTES

Protein Kinase C ε Stabilizes β-Catenin and Regulates Its Subcellular Localization in Podocytes

Michelle Duong, Xuejiao Yu, Beina Teng, Patricia Schroder, Hermann Haller, Susanne Eschenburg and Mario Schiffer

J. Biol. Chem. published online May 24, 2017
